ISSN 1464-8997 **365**

Geometry & Topology Monographs
Volume 1: The Epstein Birthday Schrift
Pages 365–381

Mutants and $SU(3)_q$ invariants

H R Morton
H J Ryder

Abstract Details of quantum knot invariant calculations using a specific $SU(3)_q$–module are given which distinguish the Conway and Kinoshita–Teresaka pair of mutant knots. Features of Kuperberg's skein-theoretic techniques for $SU(3)_q$ invariants in the context of mutant knots are also discussed.

AMS Classification 57M25; 17B37, 22E47

Keywords Mutants, Vassiliev invariants, $SU(3)_q$

1 Introduction

In previous studies of invariants derived from the Homfly polynomial, or equivalently from the unitary quantum groups, it was noted that no invariant given by a module over $SU(3)_q$ was known to distinguish a mutant pair of knots. Indeed, any quantum group module whose tensor square has no repeated summands determines a knot invariant which fails to distinguish mutants [3]. A table of invariants which fail to distinguish mutants was drawn up in [3], using this and other evidence. Direct Homfly polynomial calculations showed that a certain irreducible $SU(N)_q$ invariant, coming from the module with Young diagram $\yng(2,1)$, could distinguish between some mutant pairs for $N \geq 4$, although not for $N = 3$. These calculations also exhibited a Vassiliev invariant of finite type 11 which distinguishes some mutant pairs. The calculations left open the possibility that $SU(3)_q$ invariants might never distinguish mutant pairs.

In this paper we give details of calculations with a specific $SU(3)_q$–module which result in different invariants for the Conway and Kinoshita–Teresaka pair of mutant knots. We also consider some features of Kuperberg's skein-theoretic techniques for $SU(3)_q$ invariants in the context of mutant knots.

Much of this work was carried out in 1994–95, while the second author was supported by EPSRC grant GR/J72332.

1.1 Background

The term *mutant* was coined by Conway, and refers to the following general construction.

Suppose that a knot K can be decomposed into two oriented 2–tangles F and G as shown in figure 1.

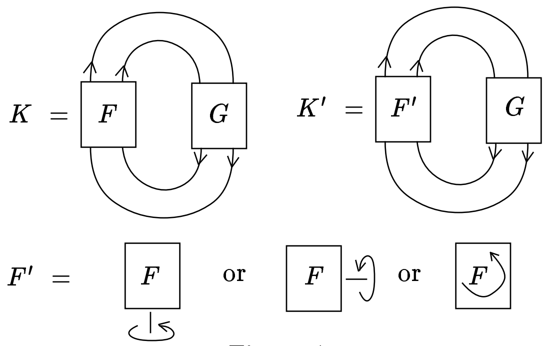

Figure 1

A new knot K' can be formed by replacing the tangle F with the tangle F' given by rotating F through π in one of three ways, reversing its string orientations if necessary. Any of these three knots K' is called a *mutant* of K.

The two 11–crossing knots with trivial Alexander polynomial found by Conway and Kinoshita–Teresaka are the best-known example of mutant knots. They are shown in figure 2.

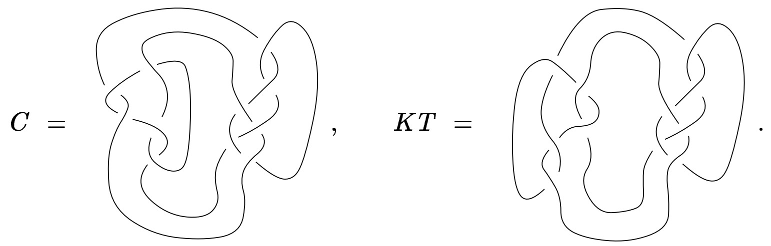

Figure 2

It is clear from figure 2 that the knots C and KT are mutants, and the consituent tangles F and G are both given from a 3–string braid by closing off one of the strings.

The simplest $SU(3)_q$ invariant not previously known to agree on mutant pairs is given by the 15–dimensional irreducible module with Young diagram .

The Homfly polynomial of the 4–parallel with $z = s - s^{-1}$ and $v = s^N$ is a sum of 4–cell invariants for $SU(N)_q$. When $N = 3$ it is known that all 4–cell invariants except that for $\yng(3,1)$ agree on mutants. Thus the Homfly polynomial of the 4–parallel, with the substitution $z = s - s^{-1}$ and $v = s^3$, agrees on mutants if and only if the $SU(3)_q$ invariant for $\yng(3,1)$ agrees on mutants.

Equally, the same substitution in the Homfly polynomial of the satellite consisting of the parallel with 3 strings, two oriented in one direction and one in the reverse direction, gives the sum of certain 4–cell invariants for $SU(3)_q$, because the dual of the fundamental module, used to colour the reverse string, is given by using the Young diagram with a single column of two cells. Then the Homfly polynomial of the 3–parallel with one reverse string, after the substitution $z = s - s^{-1}$, $v = s^3$ agrees on mutants if and only if the $SU(3)_q$ invariant for $\yng(3,1)$ agrees on mutants.

Kuperberg's combinatorial methods for handling $SU(3)_q$ invariants seemed to us for a while to offer a chance that the behaviour of $SU(3)_q$ would follow that of $SU(2)_q$. We explored the $SU(3)_q$ skein of the pair of pants, based on Kuperberg's combinatorial techniques, in the hope of proving this. An analysis of this skein is given later, as it has a geometrically appealing basis, whose first lack of symmetry again pointed the finger at the reversed 3–parallel as the first potential candidate for distinguishing some mutant pairs.

1.2 Choice of calculational method

We did not pursue the Kuperberg skein calculations for these parallels of Conway and Kinoshita–Teresaka. Although we contemplated briefly such an approach it seemed difficult to use computational aids in dealing with combinatorial skein diagrams once the number of crossings to be resolved grew beyond easy blackboard calculations, as no computer implementation of the graphical calculations in this skein was available to us.

While we could, in principle, have calculated the Homfly polynomial of the 3–parallel of Conway's knot with one string reversed there is a considerable problem in computation of Homfly polynomials of links with a large number of crossings. A number of computer programs will calculate the Homfly polynomials of general links. Mostly these rely on implementation of the skein relation, and the time required grows exponentially with the number of crossings. Such programs include those by Ochiai, Millett and Hoste. They will work up to the order of maybe 40 or even 50 crossings but slow down rapidly after that. In the application needed for this paper we have to deal with the 3–string parallel to Conway's knot with two strings in one direction and one in the other, which gives a link with 99 crossings. Even if the calculation is restricted to dealing with terms up to z^{13} only, or some similar bound, these programs are unlikely to make any impact on the calculations.

There does exist a program, developed by Morton and Short [4], which can handle links with a large numbers of crossings, under some circumstances. This is based on the Hecke algebras, but it requires a braid presentation of the link on a restricted number of strings; in practice 9 strings is a working limit, although in favourable circumstances it can be enough to break the link into pieces which meet this bound more locally. Unfortunately the reverse orientation of one string which is needed in the present case means that any braid presentation for the resulting link falls well outside the limitations of this program.

In [3] the Hecke algebra calculations on 3–string parallels with all strings in the same direction could be carried out in terms of 9–string braids, and lent themselves well to an effective truncation to restrict the degree of Vassiliev invariants which had to be calculated. The alternative possibility here of using 4 parallel strings, all with the same orientation, faces the uncomfortable growth of these calculations from 9–string to 12–string braids, entailing a growth in storage from 9! to 12! for a calculation which was already nearing its limit. There are also almost twice as many crossings (11×16), as well as a similar factorial growth in overheads for the calculations.

We consequently did not pursue Homfly calculations any further. Instead we returned to the $SU(3)_q$–module calculations and made explicit computations for the invariants of the knots C and KT when coloured by the 15–dimensional module $V_{\yng(3,1)}$, using the following scheme. This approach has the merit of focussing directly on the key part of the $SU(3)_q$ specialisation, rather than using the full Homfly polynomial on some parallel link. We give further details of the method later.

When each of the knots C and KT is coloured by the $SU(3)_q$–module $V_{\yng(3,1)}$ the two constituent tangles F and G will be represented by an endomorphism of the module $V_{\yng(3,1)} \otimes V_{\yng(3,1)}$. To calculate the invariant of the knot, presented as the closure of the composite of the two 2–tangles, we may compose the endomorphisms for the two 2–tangles, and then calculate the invariant of the closure of the composite tangle in terms of the resulting endomorphism. Let us suppose that $V_{\yng(3,1)} \otimes V_{\yng(3,1)}$ decomposes as a sum $\bigoplus a_\nu V_\nu$ of irreducible modules, where $a_\nu \in \mathbf{N}$ and $a_\nu V_\nu$ denotes the sum of all submodules which are isomorphic to V_ν. Any endomorphism then maps each isotypic piece $a_\nu V_\nu$ to itself. It is convenient to regard each isotypic piece as a vector space of the form $W_\nu \otimes V_\nu$, where W_ν has dimension a_ν, and can be explicitly identified with the space of highest weight vectors for the irreducible module V_ν in $V_{\yng(3,1)} \otimes V_{\yng(3,1)}$. Any endomorphism α of $V_{\yng(3,1)} \otimes V_{\yng(3,1)}$ maps each space W_ν to itself, and is determined by the resulting linear maps $\alpha_\nu \colon W_\nu \to W_\nu$.

Where two endomorphisms α and β of $\bigoplus(W_\nu \otimes V_\nu)$ are composed, the corresponding restrictions to each weight space W_ν compose, to give $(\alpha \circ \beta)_\nu = \alpha_\nu \circ \beta_\nu$. Now the invariant of the closure of a tangle represented by an endomorphism γ of $\bigoplus(W_\nu \otimes V_\nu)$ is known to be $\sum(tr(\gamma_\nu) \times \delta_\nu)$, where $\delta_\nu = J_O(V_\nu)$ is the quantum dimension of the module V_ν. The difference of the invariants for two knots represented respectively by γ and γ' is then given in the same way using $\gamma - \gamma'$ in place of γ.

The invariants for Conway and Kinoshita–Teresaka arise in this way from endomorphisms $\gamma = \alpha \circ \beta$ and $\gamma' = \alpha' \circ \beta$, in which α and α' represent one of the 2–tangles for Conway, and the same tangle turned over for Kinoshita–Teresaka, while the other tangle gives the same β in each case. We can write $\alpha' = R^{-1} \circ \alpha \circ R$ as module endomorphisms, where R is the R–matrix for $V_{\yng(3,1)}$. Clearly, for those ν with dim $W_\nu = 1$ we will have $\alpha'_\nu = \alpha_\nu$, and so $\gamma'_\nu - \gamma_\nu = 0$. (As noted in [3], if this happens for all ν then the invariant cannot distinguish any mutant pair). The final difference of invariants will thus depend only on those ν where the summand V_ν has multiplicity greater than 1. In the case here there are just two such ν and in each case the space W_ν has dimension 2. The calculation then reduces to the determination of the 2×2 matrices representing α_ν, α'_ν and β_ν.

1.3 Result of the explicit calculation

The difference between the values of the invariant on Conway's knot and on the Kinoshita–Teresaka knot is

$$\begin{aligned}
&s^{-80}(s^8+1)^2(s^4+1)^4(s+1)^{13}(s-1)^{13}(s^2-s+1)^3(s^2+s+1)^3\\
&(s^6-s^5+s^4-s^3+s^2-s+1)(s^6+s^5+s^4+s^3+s^2+s+1)\\
&(s^4-s^3+s^2-s+1)(s^4+s^3+s^2+s+1)(s^4-s^2+1)(s^2+1)^6\\
&(s^{46}-s^{44}+2\,s^{40}-4\,s^{38}+2\,s^{36}+3\,s^{34}-4\,s^{32}+6\,s^{30}-s^{28}-3\,s^{26}+6\,s^{24}\\
&-4\,s^{22}+4\,s^{20}+2\,s^{18}-5\,s^{16}+5\,s^{14}-2\,s^{12}-2\,s^{10}+4\,s^8-2\,s^6+s^2-1)
\end{aligned}$$

up to a power of the variable s.

This may be rewritten to indicate more clearly the appearance of roots of unity as the product of $(s^{46}-s^{44}+2\,s^{40}-4\,s^{38}+2\,s^{36}+3\,s^{34}-4\,s^{32}+6\,s^{30}-s^{28}-3\,s^{26}+$

$6\,s^{24}-4\,s^{22}+4\,s^{20}+2\,s^{18}-5\,s^{16}+5\,s^{14}-2\,s^{12}-2\,s^{10}+4\,s^{8}-2\,s^{6}+s^{2}-1)$ with the factors $(s^8-s^{-8})^2(s^7-s^{-7})(s^6-s^{-6})(s^5-s^{-5})(s^4-s^{-4})^2(s^3-s^{-3})^2(s^2-s^{-2})(s-s^{-1})^3$, and a power of s.

When this is written as a power series in h with $s=e^{h/2}$ the first term becomes $7+O(h)$ and the other factors contribute $ch^{13}+O(h^{14})$, where the coefficient c is $c=8^2.7.6.5.4^2.3^2.2$. The coefficient of h^{13} in the power series expansion of the $SU(3)_q$ invariant for the 15–dimensional irreducible module is thus a Vassiliev invariant of type at most 13 which differs on the two mutant knots.

1.4 Some background to the calculational method

In the following section we give details of the methods used in our calculations. We feel it is important that others can in principle check the calculations, as we were very much aware in setting up our initial data just how much scope there is for error. It can easily cause problems, for example, if some of the data is taken from one source and some from another which has been normalised in a slightly different way. When the goal is to show that some polynomial arising from the calculations is non-zero any mistake is almost bound to result in a non-zero polynomial even if the true polynomial is zero.

In our work here we have been reassured to find that the non-zero difference polynomial above at least has some roots which could be anticipated, since the difference must vanish at certain roots of unity. An error in the calculations would have been likely to give a difference which did not have these roots.

The computations were done in Maple, using its polynomial handling and linear algebra routines. In this way we avoided the need to write explicit Pascal or C programs for matrices and polynomials, although the computations were probably not as fast as with a compiled program. For comparison, a Maple version of the Hecke algebra program in [4] took roughly 50 times as long as the compiled Pascal program to calculate the Homfly polynomial of a variety of links when tested some time ago on the same machine.

1.5 The quantum group $SU(3)_q$

We start from a presentation of the quantum group $SU(3)_q$ as an algebra with six generators, $X_1^{\pm}$, $X_2^{\pm}$, H_1, H_2, and a description of the comultiplication and antipode. Let M be any finite-dimensional left module over $SU(3)_q$. The action of any one of these six generators Y will determine a linear endomorphism Y_M

of M. We build up explicit matrices for these endomorphisms on a selection of low-dimensional modules, using the comultiplication to deal with the tensor product of two known modules, and the antipode to construct the action on the linear dual of a known module. We must eventually determine the matrices Y_M for the 15–dimensional module $M = V_{\yng(3,1)}$ above, and find the 225×225 R–matrix, R_{MM} which represents the endomorphism of $M \otimes M$ needed for crossings.

Knowing Y_M we can find the generators Y_{MM} for the module $M \otimes M$, and thus identify the highest-weight vectors for this module. We can follow the effect of each 2–tangle F and G on the highest-weight vectors when we know how to take account of the closure of one of the strings in forming the 2–tangle from the 3–braid. To do this we need the fixed element T of the quantum group, corresponding to Turaev's 'enhancement' [6], which is used in forming the 'quantum trace'.

For the quantum groups coming from the classical Lie algebras there is a simple prescription for $T = \exp(h\rho)$ in terms of a linear form $\rho = \sum \mu_i H_i$, with coefficients determined by the Cartan matrix for the Lie algebra, [1]. In the case of $SU(3)_q$ we have $\rho = H_1 + H_2$. The quantum dimension of any module M is the trace of the matrix T_M representing the action of T on M. More generally, the effect of closing a string which is coloured by M, to convert an endomorphism of $V \otimes M$ into an endomorphism of V, can be realised by acting on M by T and then taking the partial trace of the composite linear endomorphism of $V \otimes M$. The element T is variously written as $u^{\pm 1}v$ or $u^{-1}\theta$ where v is Turaev's 'ribbon element' representing the full twist and u is constructed directly from the universal R–matrix, [7], [1].

We follow Kassel in the basic description of the quantum group from [1], chapter 17, using generators H_1 and H_2 for the Cartan sub-algebra, but with generators $X_i^{\pm}$ in place of X_i and Y_i. We use the notation $K_i = \exp(hH_i/4)$, and set $a = \exp(h/4)$, $s = \exp(h/2) = a^2$ and $q = \exp(h) = s^2$, unlike Kassel. The elements satisfy the commutation relations $[H_i, H_j] = 0$, $[H_i, X_j^{\pm}] = \pm a_{ij} X_j^{\pm}$, $[X_i^+, X_i^-] = (K_i^2 - K_i^{-2})/(s - s^{-1})$, where $(a_{ij}) = \begin{pmatrix} 2 & -1 \\ -1 & 2 \end{pmatrix}$ is the Cartan matrix for $SU(3)$, and also the Serre relations of degree 3 between $X_1^{\pm}$ and $X_2^{\pm}$.

Comultiplication is given by

$$\begin{aligned} \Delta(H_i) &= H_i \otimes I + I \otimes H_i, \\ (\text{so } \Delta(K_i) &= K_i \otimes K_i,) \\ \Delta(X_i^{\pm}) &= X_i^{\pm} \otimes K_i + K_i^{-1} \otimes X_i^{\pm}, \end{aligned}$$

and the antipode S by $S(X_i^{\pm}) = -s^{\pm 1}X_i^{\pm}$, $S(H_i) = -H_i$, $S(K_i) = K_i^{-1}$.

The fundamental 3–dimensional module, which we denote by E, has a basis in which the quantum group generators are represented by the matrices Y_E as listed here.

$$X_1^+ = \begin{pmatrix} 0 & 1 & 0 \\ 0 & 0 & 0 \\ 0 & 0 & 0 \end{pmatrix}, \quad X_2^+ = \begin{pmatrix} 0 & 0 & 0 \\ 0 & 0 & 1 \\ 0 & 0 & 0 \end{pmatrix}$$

$$X_1^- = \begin{pmatrix} 0 & 0 & 0 \\ 1 & 0 & 0 \\ 0 & 0 & 0 \end{pmatrix}, \quad X_2^- = \begin{pmatrix} 0 & 0 & 0 \\ 0 & 0 & 0 \\ 0 & 1 & 0 \end{pmatrix}$$

$$H_1 = \begin{pmatrix} 1 & 0 & 0 \\ 0 & -1 & 0 \\ 0 & 0 & 0 \end{pmatrix}, \quad H_2 = \begin{pmatrix} 0 & 0 & 0 \\ 0 & 1 & 0 \\ 0 & 0 & -1 \end{pmatrix}.$$

For calculations we keep track of the elements K_i rather than H_i, represented by

$$K_1 = \begin{pmatrix} a & 0 & 0 \\ 0 & a^{-1} & 0 \\ 0 & 0 & 1 \end{pmatrix}, \quad K_2 = \begin{pmatrix} 1 & 0 & 0 \\ 0 & a & 0 \\ 0 & 0 & a^{-1} \end{pmatrix}$$

for the module E.

We can then write down the elements Y_{EE} for the actions of the generators Y on the module $E \otimes E$, from the comultiplication formulae. The R–matrix R_{EE} representing the endomorphism of $E \otimes E$ which is used for the crossing of two strings coloured by E can be given, up to a scalar, by the prescription

$$\begin{aligned} R_{EE}(e_i \otimes e_j) &= e_j \otimes e_i, \text{ if } i > j, \\ &= s\, e_i \otimes e_i, \text{ if } i = j, \\ &= e_j \otimes e_i + (s - s^{-1}) e_i \otimes e_j, \text{ if } i < j, \end{aligned}$$

for basis elements $\{e_i\}$ of E.

We made a quick check with Maple to confirm that the matrices Y_{EE} all commute with R_{EE}, as they should. It can also be checked that R_{EE} has eigenvalues s with multiplicity 6 and $-s^{-1}$ with multiplicity 3, and satisfies the equation $R - R^{-1} = (s - s^{-1})\mathrm{Id}$.

The linear dual M^* of a module M becomes a module when the action of a generator Y on $f \in M^*$ is defined by $< Y_{M^*} f, v > = < f, S(Y_M) v >$, for $v \in M$. For the dual module $F = E^*$ we then have matrices for Y_F, relative to the dual basis, as follows.

$$X_1^+ = \begin{pmatrix} 0 & 0 & 0 \\ -s & 0 & 0 \\ 0 & 0 & 0 \end{pmatrix}, \; X_2^+ = \begin{pmatrix} 0 & 0 & 0 \\ 0 & 0 & 0 \\ 0 & -s & 0 \end{pmatrix}$$
$$X_1^- = \begin{pmatrix} 0 & -s^{-1} & 0 \\ 0 & 0 & 0 \\ 0 & 0 & 0 \end{pmatrix}, \; X_2^- = \begin{pmatrix} 0 & 0 & 0 \\ 0 & 0 & -s^{-1} \\ 0 & 0 & 0 \end{pmatrix}$$
$$K_1 = \begin{pmatrix} a^{-1} & 0 & 0 \\ 0 & a & 0 \\ 0 & 0 & 1 \end{pmatrix}, \; K_2 = \begin{pmatrix} 1 & 0 & 0 \\ 0 & a^{-1} & 0 \\ 0 & 0 & a \end{pmatrix}.$$

The most reliable way to work out the R–matrices R_{EF}, R_{FE} and R_{FF} is to combine R_{EE} with module homomorphisms cup_{EF}, cup_{FE}, cap_{EF} and cap_{FE} between the modules $E\otimes F$, $F\otimes E$ and the trivial 1–dimensional module, I, on which $X_i^{\pm}$ acts as zero and K_i as the identity. For example, to represent a homomorphism from I to $E\otimes F$ the matrix for cup_{EF} must satisfy $Y_{EF}\,\mathrm{cup}_{EF} = \mathrm{cup}_{EF}\,Y_I$, which identifies cup_{EF} as a common eigenvector of the matrices Y_{EF}, with eigenvalue 0 or 1 depending on Y. The matrices are determined up to a scalar by such considerations; when one has been chosen the scalar for the others is dictated by diagrammatic considerations. They are quite easy to write down theoretically, although to be careful about compatibility and possible miscopying it is as well to get Maple to find them in this way for itself. Once these matrices have been found they can be combined with the matrix R_{EE}^{-1} to construct the R–matrices R_{EF}, R_{FE}, R_{FF}, using the diagram shown in figure 3, for example, to determine R_{EF}. This gives

$$R_{EF} = 1_F\otimes 1_E\otimes \mathrm{cap}_{EF}\circ 1_F\otimes R_{EE}^{-1}\otimes 1_F\circ \mathrm{cup}_{FE}\otimes 1_E\otimes 1_F.$$

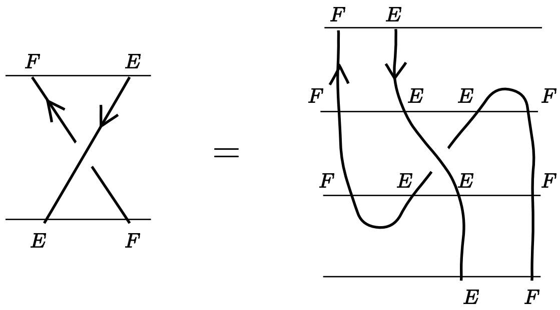

Figure 3

The module structure of $M = V_{\yng(3,1)}$ can be found by identifying M as a 15–dimensional submodule of $E\otimes E\otimes F$. We know that there will be a direct sum decomposition of $E \otimes E \otimes F$ as $M \oplus N$, and indeed that N will decompose further into the sum of two copies of a 3–dimensional module isomorphic to E and one 6–dimensional module with Young diagram ⊞. The full twist element on the three strings coloured by E, E and F acts by a scalar on each of the irreducible submodules of $E \otimes E \otimes F$. It can be expressed as a 27×27 matrix in terms of the R–matrices above. Maple can then produce a basis for each of the eigenspaces, one of dimension 15 and the other two each of dimension 6. Write P and Q for the 27×15 and 27×12 matrices whose columns are made of these basis vectors. Then P and Q give bases for M and N respectively. The partitioned matrix $(P|Q)$ is invertible. When its inverse, found by Maple, is written in the form $\begin{pmatrix} R \\ \hline S \end{pmatrix}$ we have a 15×27 matrix R which satisfies $RP = I_{15}$ and $RQ = 0$. Regard P as the matrix representing the inclusion of the module M into $E \otimes E \otimes F$. Then R is the matrix, in the same basis, of the projection from $E \otimes E \otimes F$ to M. The module generators Y_M satisfy $Y_M = R Y_{EEF} P$, giving the explicit action of the quantum group on M.

We use the injection and projection further to find the $15^2 \times 15^2$ R–matrix R_{MM}. First include $M \otimes M$ in $(E \otimes E \otimes F) \otimes (E \otimes E \otimes F)$, then construct the R–matrix for $E \otimes E \otimes F$ from the crossing of three strings each coloured with E or F over three others using the various matrices R_{EF} from above, and finally project to $M \otimes M$.

The calculations can be completed in principle from here. Represent the 3–braid in the 2–tangle F by an endomorphism of $M \otimes M \otimes M$, using R_{MM} and its inverse. Then use T_M and the partial trace to close off one string, hence giving the endomorphism F_{MM} of $M \otimes M$ determined by F. A similar calculation gives the endomorphism G_{MM}. The invariant for one of the knots is given by the trace of $T_{MM} F_{MM} G_{MM}$. The other is given by replacing G_{MM} with the conjugate $R^{-1}_{MM} G_{MM} R_{MM}$. Some calculation can be avoided by using $G_{MM} - R^{-1}_{MM} G_{MM} R_{MM}$ in place of G_{MM}, to get the difference of the invariants directly.

A considerable shortcut can be made at this point by concentrating on the effect of F_{MM} and G_{MM} on certain highest weight vectors in $M \otimes M$, rather than considering the whole of the module. A *highest weight vector* v of a module V is a common eigenvector of H_1 and H_2 (or equally K_1 and K_2) which satisfies $X_1^+(v) = X_2^+(v) = 0$. The submodule of V generated by a highest weight vector is irreducible. Its isomorphism type is determined by the eigenvalues of H_1 and H_2, which are non-negative integers. It follows easily from the relations in the quantum group that any module homomorphism $f\colon V \to W$ carries highest weight vectors to highest weight vectors of the same type.

Calculation in Maple determines the linear subspace of $M\otimes M$ which is the common null-space of X_1^+ and X_2^+. This turns out to have dimension 10, spanned by two highest weight vectors of type $(3,1)$, two of type $(1,2)$ and six further highest weight vectors each of a different type. Then the endomorphism F restricts to a linear endomorphism F_ν of the space of highest weight vectors of type ν, for each ν. We remarked earlier that weight spaces of dimension 1 will not contribute to the difference of the invariants on two mutant knots, so we need only calculate the maps F_ν and G_ν for the two 2–dimensional weight spaces $\nu=(3,1)$ and $\nu=(1,2)$. We thus choose two spanning vectors for one of these spaces and follow each of these through the 2–tangle F, taking the tensor product with M and mapping to $M\otimes M\otimes M$ as above (using repeated operations of the 225×225 R–matrix on a vector of length 225×15) before applying the matrix T_M and taking a partial trace to finish in $M\otimes M$. Since the result in each case must be a linear combination of the two chosen weight vectors it is not difficult to find the exact combination. This determines a 2×2 matrix representing F_ν for the weight space of type ν. Similar calculations for the other weight space and for G, along with a quick calculation of the 2×2 matrix representing R_{MM} on each weight type gives enough to find the contribution of each of these weight types to the difference. The final difference comes from multiplying the trace of the 2×2 difference matrix for each type ν by the quantum dimension of the irreducible module of type ν for each of the two types and then adding the results.

Up to the same power of s in each case the contribution from the weight space of type $(3,1)$ was found to be

$$\begin{aligned}
t_{31} = {} & (s^8+1)^2(s^2+1)^4(s^4+1)^3(s+1)^{13}(s-1)^{13}s^6(s^2-s+1)(s^2+s+1)\\
& (s^4-s^3+s^2-s+1)(s^4+s^3+s^2+s+1)\\
& (s^6-s^5+s^4-s^3+s^2-s+1)(s^6+s^5+s^4+s^3+s^2+s+1)\\
& (2\,s^{20}+s^{18}+s^{14}-s^{12}+2\,s^8-s^6-1)\\
& (s^{22}-s^{20}+s^{16}-2\,s^{14}+3\,s^{12}+2\,s^{10}-s^8+2\,s^6+2)\\
= {} & (2\,s^{20}+s^{18}+s^{14}-s^{12}+2\,s^8-s^6-1)\\
& (s^{22}-s^{20}+s^{16}-2\,s^{14}+3\,s^{12}+2\,s^{10}-s^8+2\,s^6+2)\\
& \times(s^8-s^{-8})^2(s^7-s^{-7})(s^5-s^{-5})(s^4-s^{-4})\\
& (s^3-s^{-3})(s^2-s^{-2})(s-s^{-1})^6s^{49},
\end{aligned}$$

and the contribution from type $(1,2)$ to be

$$
\begin{aligned}
t_{12} = \ & (s^6 - s^5 + s^4 - s^3 + s^2 - s + 1)^2 (s^6 + s^5 + s^4 + s^3 + s^2 + s + 1)^2 \\
& (s^4 - s^2 + 1)(s^8 + 1)^2 (s^4 + 1)^5 (s^2 + 1)^8 \\
& (s^2 + s + 1)(s^2 - s + 1)(s - 1)^{14} (s + 1)^{14} (s^{10} - s^8 + s^4 - s^2 + 1) \\
& (s^{18} - s^{16} - s^{14} + 2\,s^{12} - 2\,s^{10} + 2\,s^6 - 2\,s^4 - s^2 + 1) \\
= \ & (s^{18} - s^{16} - s^{14} + 2\,s^{12} - 2\,s^{10} + 2\,s^6 - 2\,s^4 - s^2 + 1) \\
& (s^{10} - s^8 + s^4 - s^2 + 1) \\
& \times (s^8 - s^{-8})^2 (s^7 - s^{-7})^2 (s^6 - s^{-6})(s^4 - s^{-4})^3 \\
& \times (s^2 - s^{-2})^2 (s - s^{-1})^4 s^{56}.
\end{aligned}
$$

The quantum dimension for the irreducible module of type $(3,1)$, which has Young diagram 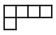, is a product of quantum integers $[6][4] = (s^6 - s^{-6})(s^4 - s^{-4})/(s - s^{-1})^2$. For the module of type $(1,2)$, with Young diagram 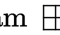, it is $[5][3] = (s^5 - s^{-5})(s^3 - s^{-3})/(s - s^{-1})^2$.

The difference between the $SU(3)_q$ invariants with the module V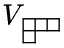 for the Conway and Kinoshita–Teresaka knots is then given, up to a power of $s = e^{h/2}$, by $[5][3]t_{12} + [6][4]t_{31}$. This yields the polynomial quoted earlier.

2 The Kuperberg skein for mutants

Let K and K' be the mutants shown schematically in figure 1. As K and K' are knots, precisely one of F or G must induce the identity permutation on the endpoints by following the strings through the tangle, while the other induces the transposition. We will consider these two cases separately.

In [2] Kuperberg gives a skein-theoretic method for handling the $SU(3)_q$ invariant of a link when coloured by the fundamental module, which he denotes by $<>_{A_2}$. Knot diagrams are extended to allow 3–valent oriented graphs in which any vertex is either a sink or a source. Crossings can be replaced locally in this skein by a linear combination of planar graphs, and any planar circles, 2–gons or 4–gons can be replaced by linear combinations of simpler pieces.

In using skein-based calculations it is helpful when dealing, for example, with satellites to regard the pattern as a diagram in an annulus, and note that it can be replaced by any equivalent linear combination of diagrams in the skein of the annulus. Thus we should consider the Kuperberg skein of the annulus, namely linear combinations of admissibly oriented 3–valent graph diagrams subject to local relations as before. A similar definition can be made for the skein of other surfaces. Notice that the relations ensure that the skein is spanned by oriented graphs lying entirely in the surface, without simple closed curves, 2–gons or 4–gons which bound discs in the surface.

In the case of the annulus this shows that the skein is spanned by unions of oriented simple closed curves parallel to the boundary of the annulus, with orientations in either direction.

When a mutant knot K is made up from two 2–tangles F and G as above then one of F and G, let us suppose G, must be a pure tangle, in the sense that the arcs of G connect the entry point at top left with the exit at bottom left, and top right with bottom right. Then K can be viewed as made from the diagram in the disc P with two holes, shown in figure 4, by embedding the planar surface P so that the two 'ears' are tied around the arcs of G. Turning the diagram in P over along the axis indicated before embedding it in the same way, and reversing all string orientations, will give one of the mutants K' of K. Any satellites of K and K' are related in a similar way, for we can view a satellite of K as constructed by decorating the diagram in P with the required pattern, and then tying the ears of P around G as before. The corresponding satellite of K' is given by turning P over, with the decorated diagram, reversing all strings, and then using the same embedding of P.

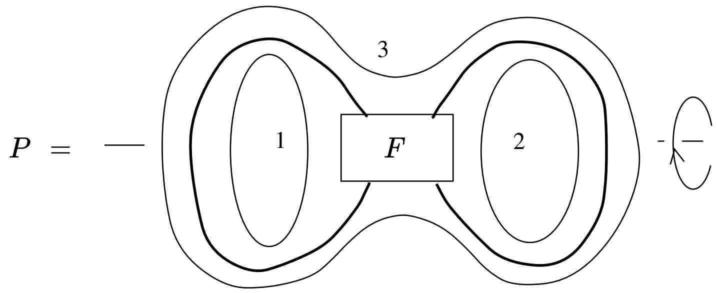

Figure 4

If we could show that the Kuperberg skein of P is spanned by elements which are invariant under turning over and reversing orientation then we could deduce that satellites of mutants such as K and K' would have the same $SU(3)_q$ invariants, by considering the decorated diagram in this skein. A proof for all mutants would need a similar analysis for the skein of the once-punctured torus, to deal with one of the other mutation operations, and the third case would then follow, using a similar argument to [5], where the truth of the corresponding results in the Kauffman bracket skein showed that satellites of mutants have the same $SU(2)_q$ invariants.

We shall now describe a basis for the Kuperberg skein of P, which has some nice symmetry properties, but not enough to give the invariance above. Indeed a diagram coming from a 3–fold parallel with one reversed string will give a linear combination of basis elements in the skein in which all but at most one pair are invariant. (Diagrams from 2–fold parallels of any orientation determine elements of the invariant subspace.)

Theorem 2.1 *The Kuperberg skein of a disc with two holes has a basis of diagrams consisting of the union of simple closed curves parallel to each boundary component and a trivalent graph with a* 2*–gon nearest to each of the three boundary components and* 6*–gons elsewhere.*

Proof Use the skein relations to write any diagram as a linear combination of admissibly oriented trivalent graphs in the surface. We can assume that there are no simple closed curves or 2–gons or 4–gons with null-homotopic boundary. There may be a number of simple closed curves parallel to each of the boundary components. The remaining graph must be connected, otherwise one of its components lies in an annulus inside the surface, and can be reduced further to a linear combination of unions of parallel simple closed curves. Consider the graph as lying in S^2, by filling in the three boundary components of the surface. It dissects S^2 into a number of n–gons, with n even, and $n \geq 6$ except possibly for the three n–gons containing the added discs. Now calculate the Euler characteristic of the resulting sphere S from the dissection by the graph. As vertices are trivalent and each edge now bounds two faces, we can count the Euler characteristic as a sum over the n–gons, in which each vertex contributes $1/3$ and each edge $-1/2$. Therefore each n–gon will contribute $1-n/6$, so the only positive contribution to $\chi(S)$ can come from 2–gons or 4–gons. These can only arise from the original three boundary components, where the maximum possible total positive contribution is 2 when each boundary component gives a 2–gon. Since the total must be 2 and the only other contributions are negative or zero, we must have three 2–gons forming the original boundary components and 6–gons elsewhere. □

If we start with a 3–parallel of a tangle F inside the planar surface P, with two strands in one direction and one in the other, and write it in the Kuperberg skein we will get a linear combination of graphs as above, each having at most 3 strings around each 'ear'. Some of these will be the union of some simple closed curves around the punctures and trivalent graphs. In figure 5 we show one such trivalent graph which fails to be symmetric under the order 2 operation of turning the surface over (and reversing edge orientations).

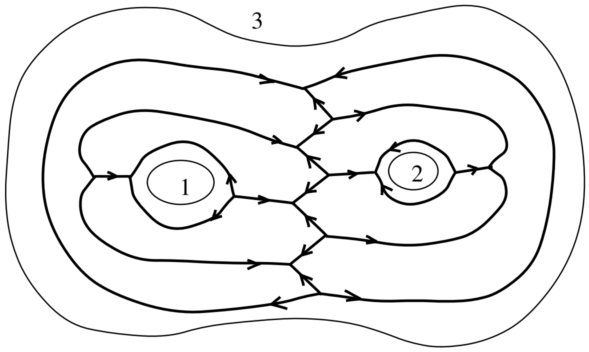

Figure 5

Note however that this graph is symmetric under the operation of order 3 in which the three boundary components are cycled. This is a general feature of the connected trivalent graphs which arise in our construction, as appears from the following description, where we replace P by a 3–punctured sphere.

We call a trivalent graph in the 3–punctured sphere *admissible* if it is oriented so that each vertex is either a sink or a source, and every region not containing a puncture is a hexagon.

Theorem 2.2 *Every admissible graph in the* 3*–punctured sphere is symmetric, up to isotopy avoiding the punctures, under a rotation which cycles the punctures. It can be constructed from the hexagonal tesselation of the plane by choosing an equilateral triangle lattice whose vertices lie at the centres of some of the hexagons and factoring out the translations of the lattice and the rotations of order* 3 *which preserve the lattice.*

Proof Let Γ be the admissible graph. By our Euler characteristic calculations we know that each puncture is contained in a 2–gon. There is a 3–fold branched cover of S^2 by the torus T^2 with three branch points, each cyclic of order 3. The inverse image of Γ in T^2 then consists of hexagonal regions, with three distinguished regions containing the branch points. This inverse image is invariant under the deck transformation of order 3 which leaves each distinguished region invariant. The further inverse image under the regular covering of T^2 by the plane is a tesselation of the plane by hexagons, and the inverse image of the centre of one of the distinguished regions determines a lattice in the plane. We want to show that this is an equilateral triangle lattice, when the hexagonal tesselation is drawn in the usual way. We need only lift the deck transformation to a transformation of the plane keeping the tesselation invariant and fixing one of the lattice points to see that it must lift to a rotation of the tesselation about the centre of a distinguished hexagon. Since the lattice is invariant under this transformation it follows that the lattice must be equilateral. The inverse image of each of the other two branch points will also form an equilateral lattice, invariant under the first rotation, and so their vertices lie in the centres of the triangles; by construction they also lie in the middle of hexagons. Although the equilateral lattice need not lie symmetrically with respect to reflections of the tesselation, as in the example shown below, it does follow that the rotation which permutes the three lattices will also preserve the tesselation. This rotation induces the symmetry of the sphere which cycles the branch points and preserves Γ. □

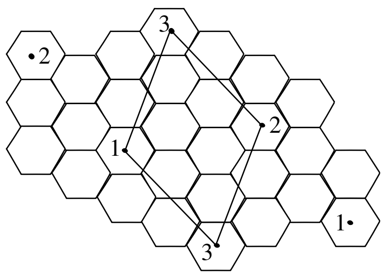

Figure 6

Figure 6 shows such an equilateral triangle lattice superimposed on a hexagon tesselation. The resulting graph in the 3–punctured sphere, whose fundamental domain is indicated, is the graph shown in figure 5 as a non-symmetric skein element in the disk with two holes. The labelling of the puncture points as 1, 2 and 3 corresponds to that of the boundary components. The 3–fold symmetry of the graph in the surface when the boundary components are cycled is evident from this viewpoint.

The Kuperberg skein of the punctured torus does not appear to have such a simple basis. The region around the puncture may be a 2–gon or a 4–gon, giving the following possible combinations: (i) a 2–gon, two 8–gons and 6–gons elsewhere, (ii) a 2–gon, one 10–gon and 6–gons elsewhere, (iii) a 4–gon, one 8–gon and 6–gons elsewhere, (iv) 6–gons only. We did not try to analyse the configurations further, in view of the results of our quantum calculations.

References

[1] **C Kassel**, *Quantum groups*, Graduate Texts in Mathematics, Springer–Verlag (1995)

[2] **G Kuperberg**, *The quantum G_2 invariant*, International J. Math. 5 (1994) 61–85

[3] **H R Morton**, **P R Cromwell**, *Distinguishing mutants by knot polynomials*, J. Knot Theory Ramif. 5 (1996) 225–238

[4] **H R Morton**, **H B Short**, *Calculating the 2–variable polynomial for knots presented as closed braids*, J. Algorithms 11 (1990) 117–131

[5] **H R Morton**, **P T Traczyk**, *The Jones polynomial of satellite links around mutants*, from: "Braids", Joan S Birman and Anatoly Libgober (editors), Contemp. Math. 78, AMS (1988) 587–592

[6] **V G Turaev**, *The Yang–Baxter equation and invariants of links*, Invent. Math. 92 (1988) 527–553

[7] **V G Turaev**, *Quantum invariants of knots and 3–manifolds*, W de Gruyter (1994)

Department of Mathematical Sciences, University of Liverpool
Liverpool L69 3BX, England

Email: `h.r.morton@liv.ac.uk`

Received: 2 September 1997